mass of the Z boson, as input of the gauge sector of the SM lagrangian, then the value of the W mass is a prediction of the model. The latter can be derived by studying the muon-decay amplitude. The radiative corrections to this process, summarized by the parameter Δr, are sensitive, through virtual loops, to the value of the masses of all the particles of the model, in particular to those of the top quark and of the Higgs boson.

The very high experimental accuracy for many EW observables has required theoretical calculations at the second order in the perturbative expansion: in particular the 2-loop corrections to the muon-decay amplitude due to the top quark [2] modify the theoretical SM prediction of the W mass of about 20 MeV and are comparable to the order of magnitude of the present experimental error. Since the W mass depends quadratically on the top quark mass, a precise experimental measurement of the former sets stringent indirect limits on the value of the latter. Unfortunately a similar pattern does not hold for the Higgs boson mass, whose dependence from the theoretical predictions of the W mass is only logarithmic. Nevertheless a global fit of all EW observables allows to set an indirect limit at the 95% C.L. for m_H = 219 GeV.

The indication that a perturbative SM Higgs boson should be relatively light has stimulated many phenomenological studies concerning the production and the decay of this boson at the LHC. The dominant production mechanism is given by the annihilation of two gluons via a top quark loop (gluon-fusion), whose amplitude is known at NNLO-QCD. Furthermore, for a value of the Higgs boson mass smaller than 150 GeV, one clean signature that will allow to study its decay is in the two photons final state. The importance of these two processes has motivated the calculation of the 2-loop NLO EW radiative corrections to the corresponding amplitudes [3]. The presence in the latter of new kinematical thresholds, due to a pair of intermediate W bosons, makes this contribution not negligible, being equal to 5-10% of the lowest order prediction and comparable with the NNLO-QCD effects. In conclusion, these processes are well under control from the diagrammatic point of view; the main source of uncertainty is due to our knowledge of the proton partonic densities.

REFERENCES
2. G. Degrassi, P. Gambino, A. Vicini, *Phys. Lett.* B383: 219-226, (1996)
3. U. Aglietti, R. Bonciani, G. Degrassi, A. Vicini, *Phys. Lett.* B595: 432-441, (2004) Phys. Lett. B600: 57-64, (2004)

Early and delayed biological effects of high energy, high linear energy transfer charged particles

D. Bettega[1], P. Calzolari[1], L. Doneda[2], M. Durante[3], L. Tallone[1]

1 Dipartimento di Fisica, Università degli Studi di Milano and INFN-Milano
2 Dipartimento di Biologia e Genetica, Università degli Studi di Milano
3 Dipartimento di Scienze Fisiche, Università Federico II, Napoli, and INFN-Napoli

Introduction

Predictions about the magnitude of the risks due to space radiation are subject to very large uncertainties (1-3) which are mainly due to poor knowledge of the induced biological effects. The components of space radiation that are of concern are high energy charged particles, expecially the high energy nuclei of heavier elements (HZE) which are a component of the galactic cosmic rays. Several reports in the literature concern the biological effects of high energy heavy ions, (4-5), but very few data regard the delayed effects of HZE particles. In this paper we report the results of a study on the relative biological effectiveness of Fe, Ti and Si-ion beams (energy range between 0.2 and 1 GeV/n) for inactivation of the proliferative capacity of human cells and of their progeny (delayed reproductive death). Reference radiation was ^{60}Co gamma rays.

Materials and methods

Inactivation of the proliferative capacity of the directly irradiated cells and of their progeny were measured in AG1522 human fibroblast cells exposed to Fe-ion beams of energies between 0.2 and 1 GeV/n, 0.97 GeV/n Ti-ion and 0.49 GeV/n Si-ion beams and, for comparison, to ^{60} Co gamma rays. The cells were maintained in α MEM medium supplemented with 20% foetal calf serum at 37 °C in 95 % air: 5% CO_2 atmosphere. In these conditions the plating efficiency was 25% and the doubling time was 24 ± 2 h. The cells were tested for mycoplasma contamination before use. Three days before irradiation 2 10^5 cells were seeded into 25 cm^2 flasks (one or two flasks for each dose). The cells were irradiated in plateau phase. After exposure the cells were harvested by trypsinization, counted, diluted and plated into 25 cm^2 flasks (five samples for each dose) at suitable numbers for colony forming assay and incubated at 37 °C. After 14 days of incubation, four flasks for each dose were fixed and stained with 10% Giemsa solution for evaluation of inactivation of the proliferative capacity (survival). At the same time one flask for each dose was trypsinized, the cells diluted and seeded at low density into five further flasks and incubated again for 14 days for the delayed reproductive assay (cloning efficiency). For both the irradiated cells and their progeny, colonies with more than 50 cells were scored as survivors and the survival linear-quadratic model was fitted to the data.

Irradiations have been performed at the Heavy Ion Medical Accelerator Center (HIMAC) of the National Institute for Radiological Sciences (NIRS) in Chiba-Japan, with 0.2 and 0.5 GeV/n Fe-ion and 0.49 GeV/n Si-ion beams, and at the NASA Space Radiation Laboratory (NSRL) in Brookhaven, with 1 GeV/n Fe-ion and 0.97 GeV/n Ti-ion beams. LET values on target were 442, 200 and 147 keV / µm for 0.2, 0.5 and 1GeV/n Fe-ion beams, 106 and 56 keV/ µm for Ti and Si–ion beams respectively. Dose rate at the sample position was around 0.25 Gy/min and 1 Gy/min at HIMAC and NSRL respectively. Cells were irradiated with various doses in the dose-range between 0.25 and 2 Gy. Irradiation with γ rays was carried out at the ^{60}Co source at the Radiotherapy Unit, Istituto Nazionale dei Tumori, Milano. Dose rate was 1.5 Gy/min and dose-range was 0.5-4 Gy.

Results and discussion

Figures 1 and 2 show surviving fraction versus dose and cloning efficiency of the progeny of the irradiated cells versus the dose given to their progenitors for all the ion- beams studied. Data with γ-rays are shown for comparison in the figures. Two to three experiments were performed with the iron ion beams and with the gamma rays. Si and Ti-ion beams data are preliminary as they were obtained by only one experiment. The curves are the best fit to the data with a linear-quadratic equation. As can be seen from Fig.1 all the heavy ion beams induce inactivation more effectively than gamma rays with the exception of the lowest energy/highest LET, 0.2 GeV/n iron ion beam, which shows at low doses the lowest effectiveness. A possible reason for this low effectiveness could be that for this LET, the mean number of particles/cell nucleus in AG1522 cells is less than 1.5 for doses up to 0.5 Gy. At low doses therefore the fraction of cells which are not traversed by any ion is not negligibile i.e. it is about 50% at 0.25 Gy. Fig.2 shows that there is a dose dependent reduction of the cloning efficiency of the progeny of the irradiated cells compared with their controls with all types of radiations. The effect is higher with all the heavy ion beams compared to gamma rays, with the 1 GeV/n Fe-ion beam being the most effective. The effect is large, indeed 14 days after the delivery of 1 Gy with the 1 GeV/n iron ion beam, the cloning efficiency relative to controls reduced to about 30%. The phenomenon of the reduction in clonogenic potential of the progeny of cells that survive radiation exposure, termed as delayed reproductive death, has been studied extensively in the literature with low LET radiations (X or gamma rays). It is generally thought that this effect, transmissible over many generations, could be due to induced genomic instability in the cell population (6-9). The results of this experiment show that, compared with gamma rays, all the heavy ion beams are highly effective in inducing delayed reproductive death i.e. the dose giving 50% delayed reproductive death is similar to that giving 50% survival in the case of 1 GeV/n Fe-ion beam, whereas the two dose values differ by a factor of about two in the case of γ-rays.

REFERENCES
1. Cucinotta, F.A., Schimmerling, W., Wilson, J.W., Peterson, L.E., Badhwar, G.D., Saganti, P.B., and Dicello, J.F., Space Radiation Cancer risks and uncertainties for Mars missions. *Radiat. Res.* 156, 682 (2001).
2. Wilson, J., Shinn, J.L., Tripathi, R.K., Singleterry, R.C., Cloudsley, M.S., Thibeault, S.A., Cheatwood, F.M., Schimmerling, W., Cucinotta, F.A., Badhwar, G.D., Noor, A.K., Kim, M.Y., Badavi, F.F., Heinbockel, J.H., Miller, J., Zeitlin, C., Heilbronn, L. Issues in deep space radiation protection. *Acta astronautica*, 49, 289 (2001)
3. Schimmerling, W., Cucinotta, F. and Wilson J.W. Radiation risk and human space exploration. Adv. Space Res. 31, 27 (2003).
4. Blakely, E. and Kronenberg, A. Heavy-Ion radiobiology: new approaches to delineate mechanisms underlying enhanced biological effectiveness. Radiat. Res. 150, S12 (1998).
5. Durante, M. Radiation protection in space. *Rivista del Nuovo Cimento* 25, 1 (2002).

Fig.1
Surviving fraction versus Dose

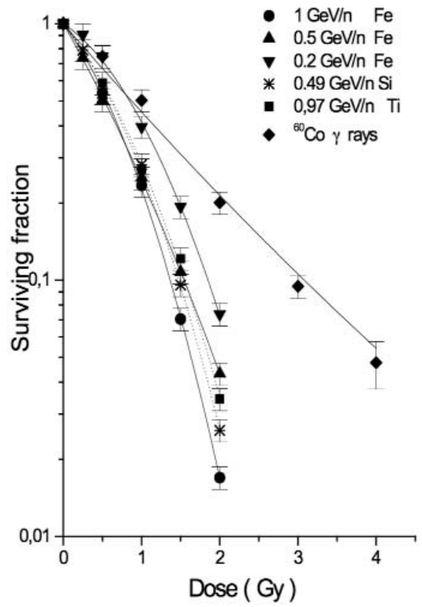

Fig.2
Cloning Efficiency of the Progeny of the irradiated cells versus dose given to the progenitors

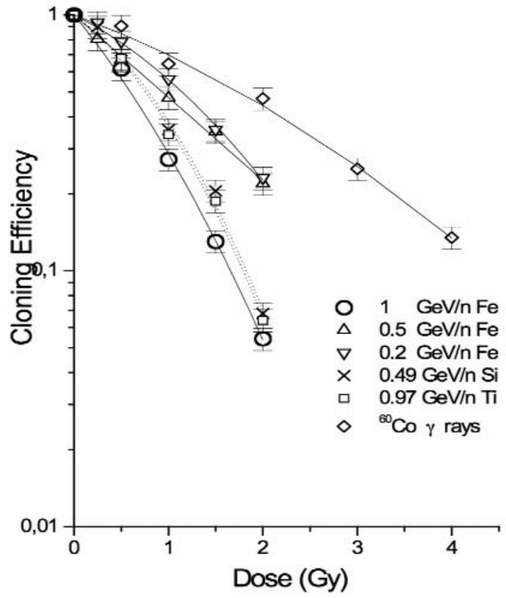

REFERENCES
6. Little, J.B. Radiation induced genomic instability. *Int. J. Radiat. Biol*. 74, 663 (1998)
7. Mendonca, M.S., Temples, T.M., Farrington, D.L. and Bloch, C. Evidence for a role of delayed death and genomic instability in radiation-induced neoplastic transformation of human hybrid cells. *Int. J. Radiat. Biol*. 74, 755 (1998).
8. Morgan, W.F., Day, J.P., Kaplan, M.I., McGhee, E.M. and Limoli, C.L. Genomic instability induced by ionizing radiation. *Radiat. Res.* 146, 247 (1996)
9. Seymour, C.B., Mothersill, C. and Alper, T. High yields of lethal mutations in somatic mammalian cells that survive ionizing radiation. *Int. J. Radiat. Biol*. 50, 167 (1986).

Relative Biological Effectiveness at low doses, RBE $_\alpha$, ($RBE_\alpha = \alpha_{ion} / \alpha_\gamma$, α_{ion} and α_γ are the linear coefficients of the dose effect curves for the ion and the gamma rays), for survival and delayed reproductive death are reported in Fig.3. RBE_α higher than one is found for both effects with all the beams with exception of inactivation due to 0.2 GeV/n iron ion beam. RBE_α is maximum in the LET interval between 140-200 keV/mm with values of 1.6 ± 0.1 and 3.3 ± 0.6 for early and delayed reproductive death respectively. RBE_α of 0.6 ± 0.1 and 1.3 ± 0.2 is found for the 0.2 GeV/n iron ion beam with LET of 442 keV/ μm for survival and delayed reproductive death respectively.

The data were also analyzed on the basis of the particle fluence (Fig. 4 and 5). A different relationship is found: the 442 keV/μm Fe-ion beam, which was the least effective for both the effects, is the most effective based on fluence, whereas the 56 keV/μm Si-ion beam shows the lowest effectiveness, i.e. for an early or delayed inactivation level of 50%, the 442 ke V/μm Fe-ion beam is about 5 fold more effective than the Si-ion beam.

Fig. 3
RBE_α versus radiation LET

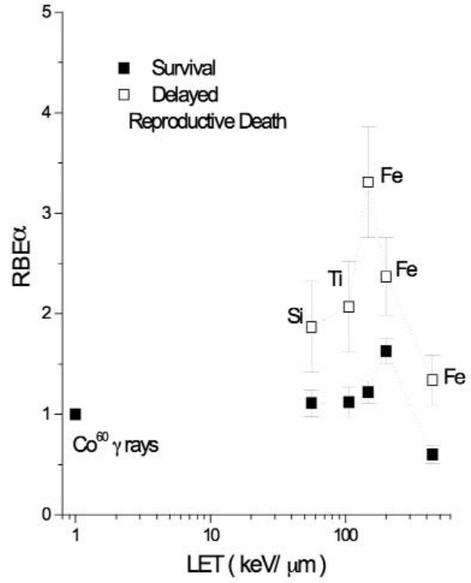

Fig. 4
Surviving fraction versus Fluence

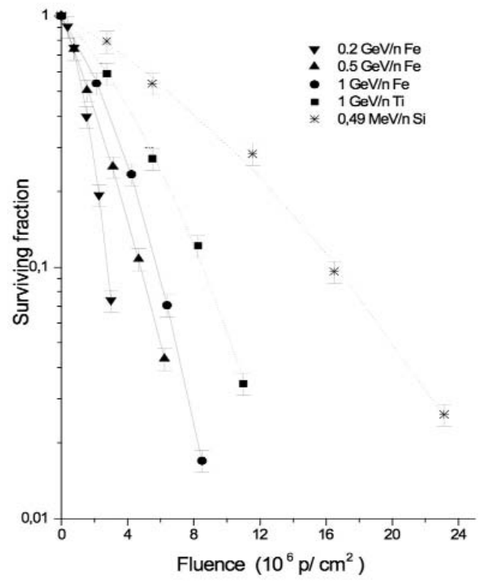

Fig. 5
Cloning Efficiency of the progeny of the irradiated cells versus Fluence given to the progenitors

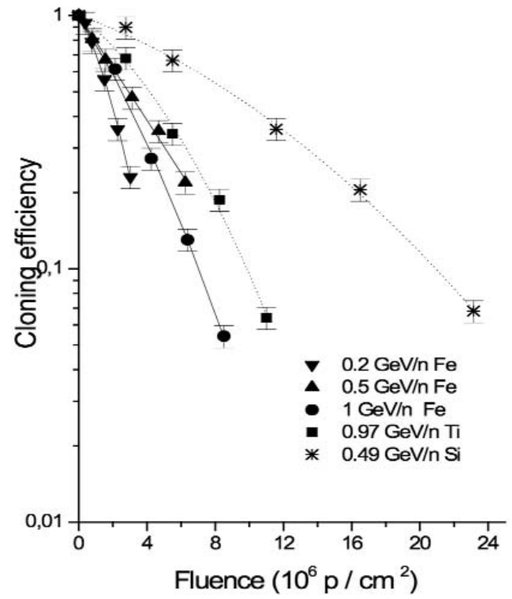

Conclusions

The results of this study show that exposure to high energy high LET ion beams induce delayed damage in the progeny of the irradiated cells in the form of reduced proliferative capacity which could indicate induced genomic instability. Compared with gamma rays, HZE particles show higher Relative Biological Effectiveness which is highest for LET values between 140-200 keV/μm and it is greater for delayed compared to early damage induction. Further studies on various delayed effects will be necessary to establish whether this result is a general phenomenon and to evaluate, if any, its consequences *in vivo*.

The results reported in this paper have been published in Advances in Space Research. 35(2):280-5, 2005.

Acknowledgements. This research project was funded by the Italian Space Agency (ASI) and by INFN

The contribution given by nuclear analytical techniques to the research in internal dosimetry

1 Dipartimento di Fisica, Sezione di Fisica Medica, Università degli Studi di Milano and INFN

M.C. Cantone[1], A. Giussani[1], and I. Veronese[1]

For a number of elements with radionuclides of significance in radiological protection, including Ru, Zr, Ce, Te and Mo, human data are poor or missing and biokinetic parameters are essentially extrapolated from data on animals. The use of stable isotopes is a publicly well acceptable and ethically justifiable method compared to the use of radioisotopes. Here is presented the developed methodology and the results obtained on volunteer subjects by using stable isotopes. The design of the investigation is taken from the standard procedure of the double tracer technique and consists in the simultaneous use of two tracers, one oral and one intravenous tracer. At different times blood samples are withdrawn, in some cases even urine is collected, and both isotopes are determined to obtain dynamical pictures of relevant processes such as intestinal absorption and the main excretion pathways. Techniques, based on activation analysis and mass spectrometry, were specifically optimised to discriminate and quantitate different isotopes of the same element in the complex matrices of the biological fluids in the order of ppb. New evidences were obtained from the direct observation on humans, which suggested modifications to be introduced in the current ICRP biokinetic models.

Introduction

The internal dose following the intake of radioactive materials cannot be measured directly and current approach adopted to provide internal dose estimates requires biokinetic models describing distribution and retention of radionuclides in selected organs and tissues. The internal dose estimates depends critically on the reliability of the biokinetic parameters used and for a number of elements with radionuclides of significance in radiological protection, including Ru, Zr, Ce, Te, and Mo, human data are poor or missing and biokinetic parameters are essentially extrapolated from data on animals. This work intends to present the contribution that basic nuclear analytical techniques, such as activation analysis and mass spectrometry, provide, presenting a well accepted and ethically justifiable approach, like the one based on the use of stable isotopes, as an alternative to the use of radioactive isotopes.

The design of biokinetic studies

The investigations on the biokinetics in humans here presented and conducted within a long dated cooperation with GSF in Munich, have been performed by using stable isotopes and by following a general design that is common in the case of radioactive isotopes. In particular the so called double tracer technique was used, that consists in the simultaneous administration of two tracers, one given orally and another intravenously, followed by the measurement of both tracer concentration in plasma and urine. At different times after the tracer administration, up to one day max, blood samples are withdrawn. Cumulated urine is collected within the first 48 h or within the first 330 h max. This approach permits to obtain dynamical pictures of relevant processes such as intestinal absorption and the main excretion pathways. Indeed, the time behaviour of the injected tracer represents the clearance from plasma, while the oral tracer concentration is the result of two competitive mechanisms: the passage to systemic circulation, that is the intestinal absorption, and the clearance itself [1]. For a better understanding of the process involved and of their significance in the absorption and distribution of the ingested elements of interest, the dependence of the absorption and of the biokinetic parameters on the chemical form, amount and composition of the ingestion was studied by using different intake conditions in volunteer subjects, according to the protocols approved by the Ethical Committee of Technical University of Munich for each of the elements investigated.

Analytical techniques

Nuclear analytical techniques, such as activation analysis and mass spectrometry, are well known methods for elemental analysis in biological samples, and both showed their ability to discriminate and quantitate different isotopes of the same element in the complex matrices of the biological fluids in the order of ppb (part per billion, μg/kg). In activation analysis nuclear

REFERENCES
1. Cantone M.C.,"Nuclear Techniques of Analysis in the Development of Biokinetic Models for Radiological Protection", *Long Range Plan, Town Meeting NUPECC, Darmstadt, Germany* (2003)

reactions are induced by bombarding the sample with projectiles of given type and energy, thus distinguishing the stable isotopes on the basis of the decay emissions of the radioactive reaction products. In mass spectrometry a series of electrical and/or magnetic fields is applied to the ionized sample, in order to discriminate between atoms or molecules with different mass to charge ratios (m/z values), thus distinguishing the stable isotopes on the basis of their nuclear mass. The widely used mass spectrometry versions (TIMS, ICP-MS) and the activation analysis by using photons, neutrons or charged particles (PAA, NAA, CPAA) have proved different performance, in relation to the matrix to be analysed and the isotopes and their amount to be determined, in terms of sensitivity and reliability. The data here reported relating to Ru, Zr and Mo investigation are obtained by using proton activation analysis in plasma sample and thermal ionization mass spectrometry in urine. In particular the stable isotopes ^{101}Ru and ^{99}Ru were used to study Ru biokinetics and the isotopes ^{96}Zr, ^{90}Zr and ^{96}Mo, ^{95}Mo respectively for Zr and Mo investigations. The procedure followed to prepare plasma samples for proton activation analysis is sketched in Fig. 1. Plasma was separated from whole blood by centrifugation and, after the addition of a known amount of an internal standard, the plasma samples are heated to dryness, powdered in an agate mortar and compressed to form a self supporting tablet. For urine sample preparation a procedure was purposely developed based on acid digestion by using a pressurized microwave decomposition. Activation of samples was performed with the proton beam of the Philips Cyclotron at the Paul Scherrer Institute in Villigen (Switzerland) up to 2002 and then with the proton beam of the Scanditronix MC 40 at the JRC in Ispra by using properly designed irradiation chambers. The used experimental conditions (energy, duration of irradiation, waiting time after EOB and counting time) are the result of a detailed optimization process [2] which is made for each one of the elements of interest to improve the minimum detectable quantity, thus to be able to maintain a reduced amount of the isotope to be ingested or injected in the investigations. The incoming proton beam energy of 19 MeV was chosen to induce predominantly the (p,n) nuclear reactions on ^{101,99}Ru, ^{96,95}Mo, ^{90}Zr and (p,2n) on ^{96}Zr, a beam intensity of 2 μA was used for a 6 sample sliding chamber and 10 μA for a 40 sample rotating chamber. After the irradiation, gamma spectrometry measurements were performed for each sample using HPGe detectors with PC based multichannel buffer cards. For instance detection limits, per gram of plasma, of 2 ng and of 1 ng for the isotopes ^{96}Zr and ^{90}Zr respectively were found for irradiation time: 40 h; cooling time: 24 h for ^{90}Zr and 30 days for ^{96}Zr; measuring time 10 h for ^{90}Zr and 3 days for ^{96}Zr and ^{90}Zr in the amount of 100 mg may be used for the injection and ^{96}Zr in the amount of 3-5 mg may be used for the ingestion.

Fig. 1
Plasma preparation procedure for activation analysis.

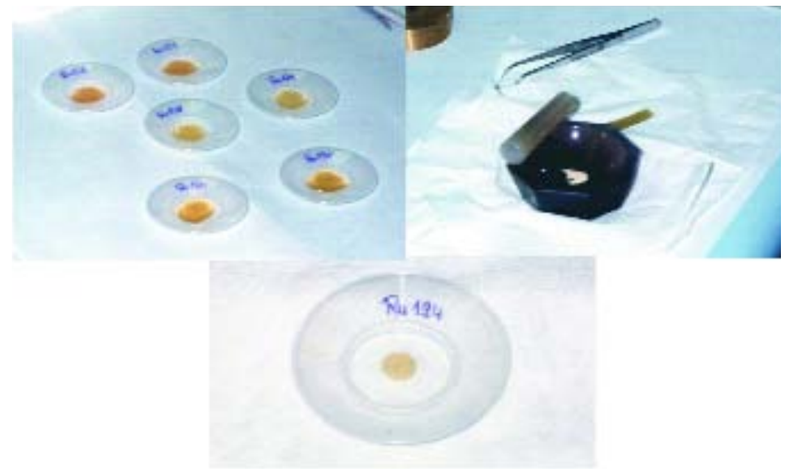

Selected results and discussion

Figure 2 shows the time course in plasma of the ^{101}Ru isotope, that is the injected tracer used in Ru biokinetic investigations. The data obtained from 6 experiments performed in three volunteers, two repeated investigations for each subject, showed intraindividual similar Ru clearance. However, this behaviour is quite different from the single exponential course adopted in ICRP model for internal dose estimates and this discrepancy can be attributable to the fact that no data on Ru clearance in humans were available before these experiments with stable isotopes.

REFERENCES
2. Veronese I., Cantone M.C., Giussani A., Maggioni T., Birattari C., Groppi F., Garlaschelli L., Werner E., Roth P., Hollriegl V., Louvat P., Felgenhauer N., Zilker Th., "Stable tracer investigations in humans for assessing the biokinetics of ruthenium and zirconium" *Radiation Protection Dosimetry* 105, 209 (2003)

Figure 3 shows the results obtained in one of the three subjects investigated to study the influence of the chemical form on the plasma clearance of Ru in humans. In this investigation Ru was injected in form of citrate Ru complexes (organic) and in a second experiment, performed on the same subject, Ru was injected in inorganic form [3]. The time behaviour of Ru concentration in plasma in the two experiments, shows that organic form is cleared from the plasma very rapidly, while the inorganic Ru remains longer in the systemic circulation. These findings are also confirmed by the renal excretion patterns. Indeed, as shown in the upper part of the same figure, the urinary excretion for the organic Ru is high, more than 50 % in the first 24 h, while the inorganic Ru is excreted only about 25% in the 48 h.

Figure 4 shows, in one of the subjects investigated for Zr study, the time course of the percentage concentration for both the injected and ingested tracer and in particular the results of two independent investigations on the same subject are here reported [4]. The red curves represents the current predictions for Zr on the basis of ICRP models and the black curves are the result of fitting a modified model to the whole set of data. In comparison to ICRP predictions a faster absorption is found which is 4 times lower than the recommended value for members of the population. Differences in the value of intestinal absorption can have consequences on the calculation of dose and more significantly can be relevant when using the model for the interpretation of urine measurements after accidental incorporation to assess retrospectively intake and dose.

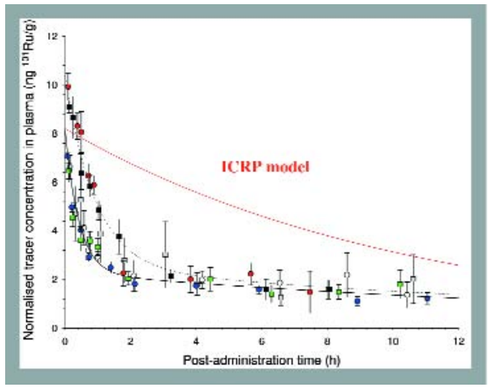

Fig. 2
Time courses of the injected Ru isotope. Two experiments for cach of the three subject investigated.

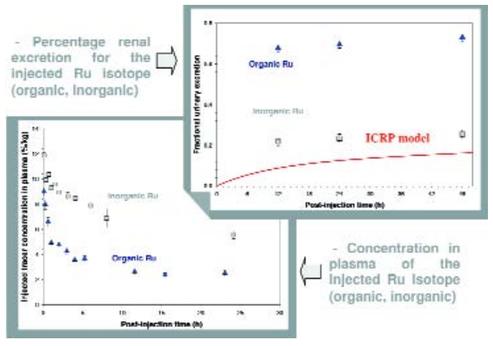

Fig. 3
Time behaviour in plasma and in urine of Ru injected tracer in two different chemical form (organic and inorganic).

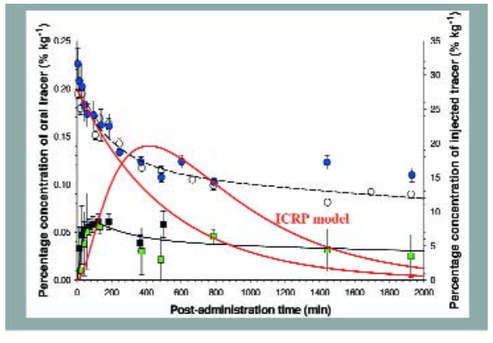

Fig. 4
Percentage concentration of ingested and injected Zr isotopes in one investigated subject.

REFERENCES
3. Veronese I., Giussani A.,Cantone M.C., Birattari C., Bonardi M., Groppi F., Hollriegl V., Roth P., Werner E., "Influence of the chemical form on the plasma clearance of ruthenium in humans" *Applied Radiation and Isotopes* 60, 1, 7 (2004)
4. Veronese I., Giussani A., Cantone M.C., Maggioni T., Birattari C., Groppi F., Werner E., Roth P., Hollriegl V., "A re-evaluation of the biokinetics of zirconium in humans" *Applied Radiation and Isotopes* 58, 4, 431 (2003)

Figure 5 shows, as an example, the data of repeated investigations, on one subject, following different ingestion conditions. In the investigations the ingestion of different Mo amounts, in liquid and solid form, the use of intrinsic and extrinsic tag and the ingestion of black tea, as inhibitor of absorption, together with Mo, are included. These data are taken from a series of 63 studies on Mo biokinetics performed with 17 volunteers [5]. A number of considerations can be obtained from the different behaviours shown in the figure. It is evident that intestinal absorption is almost complete for aqueous solution, while decreases with increasing amount of ingestion and in the case of solid meal and this fact calls for definition of a separate set of parameters for liquid and solid ingestion. On the basis of the whole set of results the biokinetic model recommended by ICRP was upgraded and different sets of fractional transfer rates were proposed for liquid and solid ingestion. Dose per unit intake were calculated according to ICRP guidelines but using the revised model. Considerable deviations were observed for the dose to selected organs. For example, Fig. 6 shows the relative contribution of each organ/tissue to the committed dose after ingestion of ^{99}Mo (66 h half life) according to the ICRP models, where no distinction is taken between solid and liquid ingestion, and the relative contributions calculated by using the revised model based with separate parameters for liquid ingestion and for solid ingestion. For example, the dose per unit intake for colon, after ingestion of ^{99}Mo in solid form resulted about 7 times higher than the ICRP value, and consequently the relative contribution to the total dose is evidently different. This fact could be of importance with respect to deterministic effects to particularly radiosensitive organs.

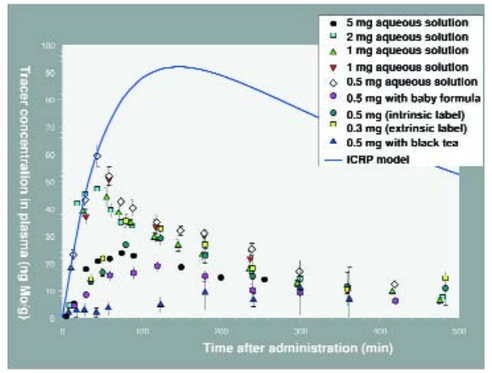

Fig. 5
Percentage concentration of ingested Mo in one subject, under different ingestion conditions.

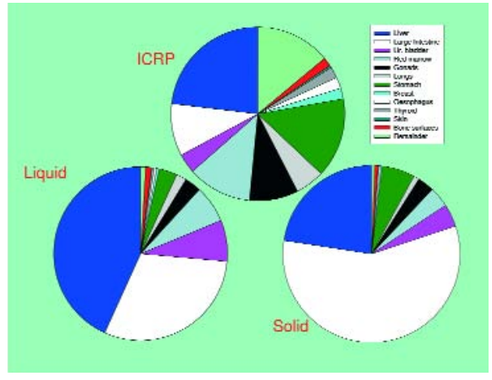

Fig. 6
Relative contributions of each target organ/tissue to the committed dose due to ^{99}Mo ingestion, as given by ICRP and as calculated by using the revised model with separate set of parameters fro liquid and solid ingestion.

Conclusions

The use of stable isotopes as tracers, in combination with a suitable technique of analysis, such as activation with protons, has allowed obtaining biokinetic data for element of interest in radiological protection directly in healthy human subjects. The results of the tracer studies have filled a gap in the current knowledge proving information about kinetics of intestinal absorption and of blood plasma clearance that were previously not available or only based on experiments on animals. These new pieces of information have indicated a series of modifications that can be introduced in the current ICRP models towards a better confidence in internal dose estimates.

REFERENCES
5. Giussani A., Arogunjo A.M., Cantone M.C., Tavola F., Veronese I., "Rates of intestinal absorption of molybdenum in humans" *Applied Radiation and Isotopes* in press (2006)

Role of physics in a 'Trojan horse' method for radiotherapy

1 Dipartimento di Fisica, Università degli Studi di Milano and INFN

G. Gambarini[1]

1. Introduction

Slow neutrons have shown promising potentiality for treating diffuse or radio-resistant tumours. The energy delivered by slow-neutron interactions with tissue components is relatively low. On the opposite, if a drug containing suitable isotopes with high cross section for thermal neutrons can be concentrated in tumour tissue, then thermal neutron reactions release high energy in tumour tissue itself. This kind of radiotherapy was initially known as "Trojan horse" method. Boron neutron capture therapy (BNCT) takes advantage of the possibility of selectively accumulating the isotope ^{10}B in tumour cells and of the high cross section of the reaction with thermal neutrons

$$^{10}B(n,\alpha)^{7}Li \ (\sigma = 3837 \text{ b}).$$

The short range in tissue of the emitted α and ^{7}Li particles (<10 μm) allows localised energy release in tumour cells, saving the surrounding healthy tissue. Therefore, BNCT is of particular interest for diffused tumours, such as liver tumours. Moreover, owing to the high linear energy transfer (LET) and relative biological effectiveness (RBE) of α and ^{7}Li particles, BNCT is potentially effective for radio-resistant tumours, such as multiform glioblastoma and some kinds of melanomas. Very promising results have been obtained in trials on patients with glioblastoma or liver cancer. Interdisciplinary research is still carried out aimed at setting up suitable modalities for BNCT, in particular for achieving higher selectivity of the boron carrier (Chemistry and Biology), good quality of neutron fields (Nuclear Engineering and Physics) and reliable dosimetry methods (Physics).

2. Dosimetry for BNCT

As known, neutrons are not directly ionising particles. Then, during the exposure of a patient to thermal or epithermal neutrons, the absorbed dose in tissue is released by the various components of secondary radiation. For BNCT treatment planning, besides the radiotherapy dose in tumour tissue with accumulation of ^{10}B, it is necessary to evaluate the dose delivered by thermal and epithermal neutrons to healthy tissue too, because this information is necessary to establish the maximum neutron fluence admitted for the treatment. The reactions mainly responsible of the released energy in tissue or tissue-equivalent materials are:

$$^{1}H(n,\gamma)^{2}H \ \ (\sigma = 0.33 \text{ b})$$

whose γ-rays (of 2.2 MeV) can travel many centimetres through tissue, and

$$^{14}N(n,p)^{14}C \ (\sigma = 1.81 \text{ b})$$

whose emitted protons (of about 0.6 MeV) have short range in tissue and give local dose deposition. Moreover, epithermal and fast neutrons undergo elastic scattering (mainly with hydrogen) so that recoil nuclei also contribute to the absorbed dose. The spatial trends and the relative contributions to the total absorbed dose of such secondary components depend on neutron energy spectrum, on beam geometry and on the size and dimension of the irradiated volume. Owing to the different LET and RBE of the various kinds of secondary radiation, the various dose components have to be separately identified.

A method has been developed for imaging the various dose components in phantoms exposed in thermal or epithermal neutron fields suitable for BNCT. The method is based on optical imaging of suitably designed gel dosimeters, properly made up in the laboratory, that act as continuum dosimeters and allow achieving images of the absorbed dose. Dosimeter analysis consists in measurements of visible light transmission, imaged by means of a CCD camera. A gel dosimeter after irradiation in a BNCT phantom exposed in a reactor epithermal column is shown in Fig. 1. Gel dosimeters are particularly convenient for performing dose measurements in thermal or epithermal neutron fields. In fact, they have good tissue-equivalence for neutrons of whichever energy and also for the secondary radiation generated by neutron interactions. Moreover, it is possible to suitably design gel matrices with different elemental compositions so that the differential analysis of the responses of dosimeters with different isotopic content permits the various secondary-radiation components to be distinguished [1,2]. The method for separating the dose contributions, proposed and studied in the laboratory, consists in introducing, into the phantom of interest, coupled layers of gel dosimeters with a composition differing for the content of one isotope whose reaction with neutrons gives production of charged particles. The separation of dose contributions is obtained by pixel-to-pixel manipulations of the detected images, utilizing suitable procedures and algorithms. The images of thermal neutron fluence are obtainable too, by elaborating the images of the dose due to the charged particles emitted in the reactions of thermal neutrons with ^{10}B. Such particles, in fact, release their energy locally and then the thermal neutron fluence can be attained utilising kerma factors.

In order to study the reliability of the proposed method, experiments have been carried out at the fast research reactor Tapiro (ENEA, Casaccia, Rome), shown in Fig. 2, in the thermal and epithermal columns properly designed for BNCT research. In order to check the correctness of the obtained results, dose and fluence profiles have been extracted from images and their trend has been compared with the results obtained in a few positions by means of other dosimetry techniques. A suitable method for mapping gamma-dose and thermal neutron fluence with thermoluminescent dosimeters (TLD) has been developed in the laboratory [3]. Besides TLDs, also activation techniques and Monte Carlo calculations have been utilised for intercomparison of data. The consistency of the results obtained with the various methods has confirmed the reliability of the proposed procedure.

Fig. 1
Gel dosimeter after irradiation in a phantom exposed to a reactor epitermal neutron beam.

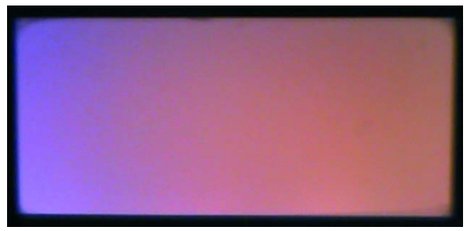

Fig. 2
Tapiro reactor of ENEA (Casaccia, Rome).

REFERENCES
1. Gambarini G., Birattari C., Colombi C., Pirola L. and Rosi G., "Fricke-Gel Dosimetry in Boron Neutron Capture Therapy", Radiation Protection Dosimetry 101, 419 (2002)
2. Gambarini G., Colli V., Gay S., Petrovich C., Pirola L., and Rosi G., "In-phantom imaging of all dose components in boron neutron capture therapy (BNCT) by means of gel dosimeters", Applied Radiation and Isotopes 61, 759 (2004)
3. Gambarini G., Klamert V., Agosteo S., Birattari C., Gay S., Rosi G., and Scolari L., "Study of a method based on TLD detectors for in-phantom dosimetry in BNCT", Radiation Protection Dosimetry 110, 631 (2004

The method of gel dosimetry in neutron fields has encountered international interest, and experiments are now in development at nuclear reactors in other research centers where BNCT trials of patients have been performed. Besides Tapiro reactor, present experiments are mostly carried out at the TRIGA reactor of Pavia University, now recognized from the BNCT community in all the world owing to a successful treatment of human liver, at the HFR (high flux reactor) of the European Joint Research Center of Petten (Holland), that is the first European BNCT unit performing treatment of human patient, and at the LVR-15 reactor of Rez (Prague) where BNCT is studied and experimented from many years.

3. Some results

In Fig. 3, the total dose in the central plane of a phantom for BNCT experimentation is shown. The phantom was exposed in the epithermal column of TAPIRO reactor, up to a fluence of about 10^{13} cm^{-2} s^{-1}. The contributions to the total dose are from photons, from α and ^{7}Li charged particles emitted in ^{10}B reactions and from fast neutrons. In Fig. 4 the results of the separation of the therapy dose due to ^{10}B reactions and the photon plus fast neutron doses are reported. Photon and fast neutron doses have been separated too, with a method based on cou-

ples of gel layers having the same composition but obtained one with water and the other with heavy water [4]. In Fig. 5, results of such separation are shown. Here depth dose profiles in the central axis of the phantom have been extracted from images, and compared with the results of TLD measurements and of Monte Carlo calculations. All dose profiles, extracted from dose images, are reported in Fig. 6.

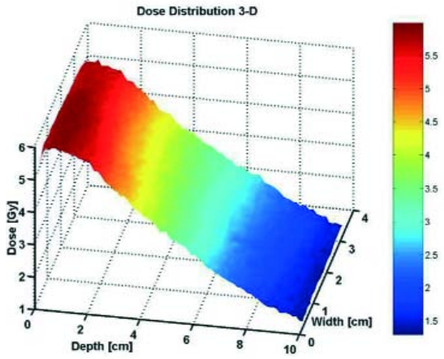

Fig. 3
Total dose in the central plane of a phantom for BNCT experiment, exposed to Tapiro epithermal beam.

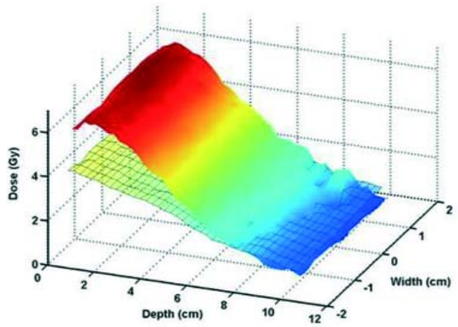

Fig. 4
Images of the therapy dose due to ^{10}B reactions and the photon plus fast-neutron doses.

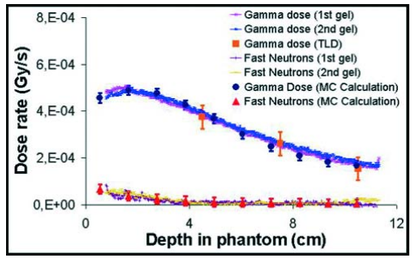

Fig. 5
Result of separation of photon and fast-neutron doses.

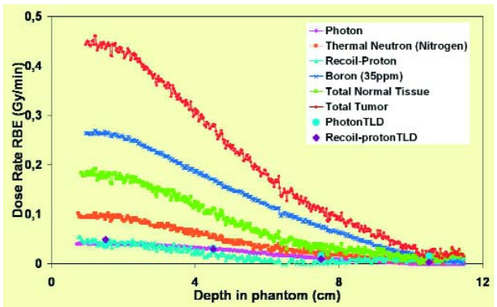

Fig. 6
Profiles of all the contributions to the absorbed dose along the central axis of the phantom exposed in the Tapiro epithermal column.

4. Final remarks

The proposed method has shown substantial potentialities. At present, no other method allows obtaining spatial images of all dose contributions in thermal or epithermal neutron fields.

REFERENCES
4. Gambarini, G., Agosteo, S., Danesi, U., Garbellini, F., Lietti, B., Mauri, M., Rosi, G., "Imaging and profiling of absorbed dose in neutron capture therapy", IEEE Trans. Nucl. Sci. 48, 780–784 (2001).

Production of non-conventional high specific activity radionuclides for biomedical, toxicological and environmental purposes

F. Groppi[1], M.L. Bonardi[2], S. Morzenti[3], E. Persico[4], L. Gini[5], E. Menapace[2], Z.B. Alfassi[3], B.L. Zhuikov[4], K. Abbas[5], and U. Holzwarth[5]

1 LASA, Dipartimento di Fisica, Università degli Studi di Milano and INFN
2 Divisione per le Tecnologie Fisiche Avanzate, ENEA, Bologna, Italy
3 Department of Nuclear Engineering, Ben Gurion University, Beer Sheva, Israel
4 Institute for Nuclear Research of Russian Academy of Sciences, Moscow, Russia
5 Institute for Health and Consumer Protection, Joint Research Centre, EC, Ispra (Va), Italy

Low- and medium-energy accelerators and sometimes thermal nuclear reactor, allow production of very high specific activity radionuclides (HSARNs) for biomedical, environmental, toxicological and occupational investigations. Specific Activities of the order of GBq·μg^{-1} are achieved; this means that the experiments can be carried out in the sub-nanogram range (nanochemistry). The HSARNs allow labeling increasing amounts of different chemical forms of toxicological or pharmacological interest, with the possibility to obtain dose vs. effect relationships on both cell cultures and laboratory animals. In nuclear medicine, "very high" A_S - in No Carrier Added radiopharmaceuticals - are normally required to avoid undesirable effects due to high chemical concentration of labeled species. Some labeled species are sparingly soluble in body fluids, organs and barrier membranes; some others present toxic or adverse effects onto humans; a low A_S(NCA) means a high molar concentration and could interfere into normal human metabolism, by inducing undesired pharmacological effects. High-resolution HPGe χ-spectrometry and β-spectrometry by liquid scintillation counting allow determination of radionuclidic and radiochemical purities of the tracer and determination of radiochemical yield of processing procedures. Chemical purity determination is carried out by a range of analytical and radioanalytical techniques. Radionuclide production for biomedical applications has been brought up in the years, at LASA, particularly in co-operation with JRC-Ispra of EC and LENA-Pavia.

Introduction

Specific Activity, Activity Concentration and Isotopic Dilution Factor: Specific Activity (A_S) of a radionuclide (RN), is defined as the ratio between the activity of the stated RN to the mass of "isotopic carrier" present in the sample, i.e. in the SI units this quantity is given in Bq.kg^{-1}, or in most practical cases GBq·μg^{-1}. With the term "isotopic carrier", we mean the total amount of both stable and radioactive atoms of same Z present in the sample. A_S must not be confused with the "activity concentration" C_A, that is the activity of a stated RN to the mass or (volume) of substrate where the RN is diluted in; in the SI, C_A has the same units of A_S. The A_S of a RN, if no other RNs of the same Z are present, is named Carrier Free, A_S (CF). This quantity is an *intensive parameter* that depends on the physical properties of RN only, in accordance to the definition: $A_S(CF) = N_{Av}·\lambda·M^{-1}$ where: N_{Av} is the Avogadro's constant and M is the atomic mass of the RN. This parameter is a physical constant, not depending on either decay time or chemical or physical environment. The higher is M the lower is A_S(CF); conversely, the shorter is the half-life of the RN, the higher is A_S. Actually, the atomic mass of different RNs of Periodic Table from medium to high Z varies of less of one order of magnitude, while the half-life is the parameter that determines the order of magnitude of A_S(CF). In practice, the Carrier Free condition can be achieved in a few selected cases.

It is useful to derive a further non-dimensional quantity (always > 1), the Isotopic Dilution Factor (IDF), defined as: IDF = (mass of isotopic carrier)/(mass of RN) = $A_S(CF)·A_S^{-1}$. In order to optimize radionuclidic purity increasing at the same time A_S of light ion produced radionuclides, two main approaches must be considered. A. An accurate knowledge of "experimental" excitation functions of nuclear reactions involved, as a function of projectile energy, as well as the knowledge of the excitation functions of both "stable" and radioactive nuclides produced by side reactions, that are isotopic with the RN of interest; B. the optimization of very selective radiochemical separations of radionuclide produced, without "intentional" addition of either isotopic or even isomorphous/iso-dimorphous carrier. The radionuclides and labeled compounds obtained in this way are named No Carrier Added (NCA). Figure 1 reports the different definitions of A_S. Even without "intentional" addition of "isotopic carrier", the contamination by isotopic carrier is unavoidable and it is due to chemical impurities present in both target materials, target holders, chemicals used during radiochemical processing and even by contact of a HSARN with the polluted environment. Whenever the radiotrac-

REFERENCES
1. Bonardi M., Groppi F., and Mainardi H.S., "High Specific Activity Radioactive Tracers: a powerful tool for studying very Low Level and Long Term Exposure to different Chemical Forms of both Essential and Toxic Elements", *Microchemical Journal*, 73 (2002) 153.
2. Menapace E., Birattari C., Bonardi M.L., and Groppi F., "Experimental results and model calculation of excitation functions relevant to the production of specific radioisotopes for metabolic radiotherapy and for PET", *Radiation Physics and Chemistry*, 71 (2004) 493.
3. Bonardi M.L., Groppi F., Mainardi H.S., Kokhanyuk V.M., Lapshina E.V., Mebel M.V., and Zhuikov B.L., "Cross section studies on Cu-64 with zinc target in the proton energy range from 141 down to 31 MeV", *Journal of Radioanaytical Nucear Chemistry*, 264 (2005) 101.

er is used to label any chemical compound or radiopharmaceutical, the "isotopic carrier" is easily introduced into the sample by the labeling procedure. Finally, if in order to administer a radiopharmaceutical or labeled compound, use is made of a physiological medium or metallic injection needles, the sample is contaminated in principle by any element present in the Periodic Table, excluded a few "artificial" ones. A complete scheme showing the different steps that must be followed for reaching these results and achieve very high purity radionuclides and labeled compounds is reported in Fig. 2. In Fig. 3 are reported the main uses of HSARNs.

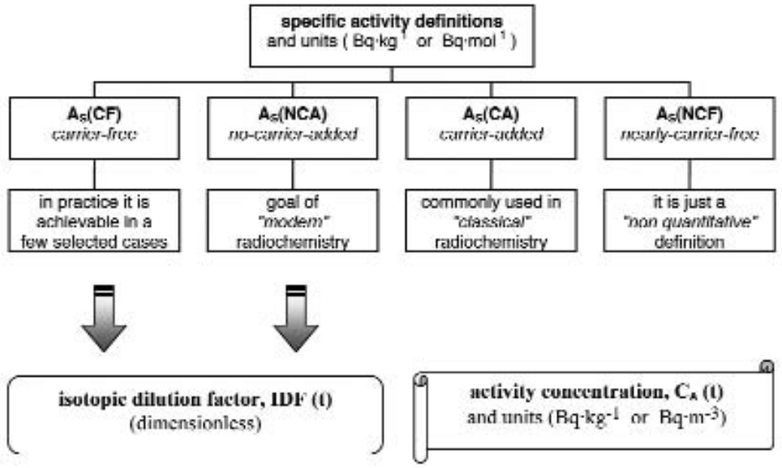

Fig. 1
Different definitions of specific activity S_A(NCA) for radionuclides and labeled compounds. The concept of isotopic dilution factor IDF is related to the definition of S_A(t), while the activity concentration C_A(t) has a completely different meaning.

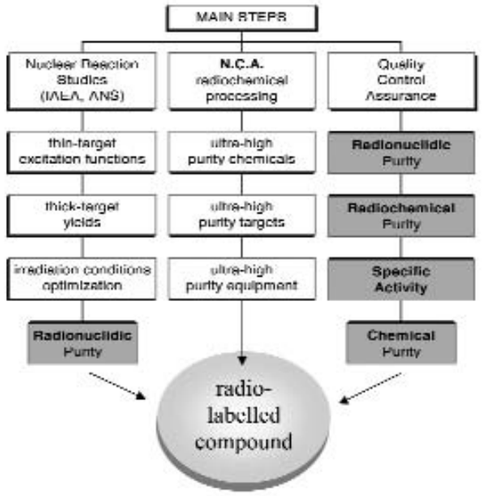

Main steps in cyclotron and nuclear reactor production of HSARNs and labelled compounds. Collaboration with international organisations is mandatory: IAEA, International Atomic Energy Agency, Nuclear Data Section, NDS, Vienna, Austria and ANS, American Nuclear Society, La Grange Park, Illinois, USA.

Fig. 2
Mains steps in cyclotron and nuclear reactor production of HSARNs and labelled compounds. Collaboration with international organisations is mandatory: IAEA, International Atomic Energy Agency, Nuclear Data Section, NDS, Vienna, Austria and ANS, American Nuclear Society, La Grange Park, Illinois, USA.

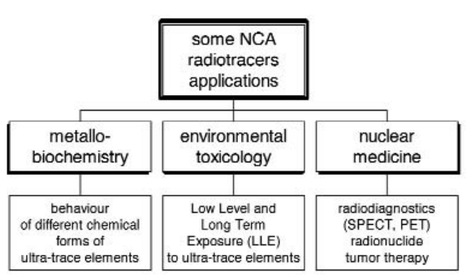

Fig. 3
Main modern applications of High Specific Activity Radionuclides in No Carrier Added form.

Experimental activity

Since the beginning of the 70's, a large range of HSARNs, have been produced at former Cyclotron Laboratory of the UNIMI. Several nuclear data for radionuclide production, measured in our Laboratory, are presently recommended by the Nuclear Data Section of IAEA, Vienna. More recently, use is made of the Cyclotron of JRC-Ispra, and the research Nuclear Reactor of the University and CNR of Pavia. Several International institutions are involved (Canada, Hungary, Israel, Russia, USA).

The Isotopic Carrier has two origins:

1. it is introduced into the sample by isotopic impurities present in both target materials, environment and chemicals used for radiochemical processing of the RN;
2. it is produced by side nuclear reactions and decay chains leading to both stable and radioactive isotopes of the same element (same compound). Thus, the nuclear reaction route and radiochemical processing procedure chosen are fundamental steps to gain HSARNs.

Reagents and chemical equipment

High purity water of Type I was produced with Millipore equipment supplied with deionised water obtained from a mixed-bed twin ion-exchange column. A total oxidable carbon (TOC) value of 10 ppb is achieved. All equipment are made by Teflon-PFA, for operations at temperature up to 200 °C. At higher temperature use is made of quartz-ware of nuclear grade. All the acids and organic chemicals are analysed for metal impurities by graphite-furnace atomic absorption spectrometry (GF-AAS), inductively coupled plasma optical-emission spectrometry (ICP-OES), instrumental neutron activation analysis (INAA) and by high-resolution γ spectrometry. Concentrated metal standard solutions are diluted as required for the standard additions and for method evaluation, by both GF-AAS, ICP-OES and INAA. All ion exchange resins used are of analytical grade purity. Suitable portions of resins are preconditioned by swelling either in high purity water, buffer or acidic solution and then filled into polypropylene columns and repeatedly washed, up to reach a constant pH value of the eluate. For some chemical separation and quality control, use is made of inorganic ion exchangers. All chromatographic fractions are collected in disposable plastic vials for both γ and β spectrometry.

Nuclear data traceability and isotope nomenclature

All nuclear data are treated in accordance with the IAEA recommendations. Whenever it is possible, the official IUPAC nomenclature and the SI are adopted.

Instrumentation

Nuclear activations are carried out at the compact cyclotron of JRC-Ispra of EC, as well as at the TRIGA thermal nuclear reactor of University and CNR Pavia. The accelerator (K–38) gains proton and alpha beams, with energy variable up to 38 MeV, as well as deuteron beams of energy up to 19 MeV. The nuclear reactor is a 250 kW research reactor, with 30 % enriched ^{235}U fuel rods. A thermal nuclear flux density varying from 10^{16} to 9 10^{16} $n \cdot m^{-2} \cdot s^{-1}$ is used in different cases (INAA and isotope production). The epithermal component of neutron spectrum was experimentally measured by Cd shielding and is less than 10%.

High-resolution gamma spectrometry is performed by four 50 cm^3 coaxial HPGe detectors, with intrinsic efficiency of 15%, with a peak to Compton ratio of 30 to 1 at 1 333 keV, FWHM 2.3 keV, connected to spectroscopy amplifiers and A/D 2 x 4096 MCAs. The spectroscopy amplifiers are set to gain a channel/energy conversion factor 2:1. Gamma spectra in the energy range up to 2 000 keV were acquired and analyzed by advanced s/w packages. The efficiency data, obtained by certified point sources of ^{152}Eu, ^{226}Ra and ^{133}Ba, are fitted by advanced s/w packages.

Beta spectrometry by liquid scintillation counting (LSC), is performed by a 1k MCA Liquid Scintillation Counter, with: three energy window, random coincidence monitor and Horrocks Number quenching correction capabilities. Large activities were measured by a well type ionisation chamber dose calibrator.

Metal determinations are performed with GF-AAS, ICP-OES, for most elements. Moreover, for some particular metals we use INAA, even if this technique could deter-

mine at least 35 trace elements simultaneously. Some irradiated targets are mineralized by a microwave digestion system. Some trace metal determinations are performed by anodic and cathodic stripping voltammetry too. For most elements an inter-comparison between the different analytical techniques is carrier out.

Specific activity determination

In most cases, in order to determine the experimental value of NCA Specific Activity, we use radiometric techniques, like γ and β spectrometry hyphenated with elemental analysis techniques, like GF-AAS, ICP-OES, NAA and ASV.

Nuclear reaction choice, energy threshold, Coulomb barriers

The choice of more suitable nuclear reaction for production of each specific RN is based on a preliminary study. Q values, energy thresholds for a charged particle on a target and Incoming particle Coulomb Barrier are calculated by the mass defects with kinematics in the laboratory system.

In a few selected cases, use is made of neutron-induced nuclear reactions in thermal nuclear reactor. This method leads to HSARNs only when the RN produced decays on the RN of interest by negatron decay: in this case the RN can be radiochemically separated from irradiated target. Otherwise, NAA is used for elemental chemical analysis of RN produced.

Conclusions

Medium energy cyclotron and sometimes nuclear reactors, allow production of HSARNs for biomedical, environmental, toxicological and occupational studies about long-term exposure to low doses of ultra-trace elements present in the ecosystems. Specific activities of the order of GBq·μg^{-1} are achieved, so the experiments can be carried out in the sub-nanogram concentration range.

HPGe γ spectrometry, allows both qualitative and quantitative analytical and radioanalytical investigations on activated targets and radiochemical fractions. Conversely, β spectrometry by LSC is intrinsically characterised by low-resolution capability, due to continuous spectra of beta emitters, but presents a very high counting sensitivity. After the End Of Chemical Processing of target itself, β spectrometry can be used effectively to follow either β or electron decay of pure RN. Elemental analysis techniques like AAS, ICP-OES, INAA, RNAA, ASV, allow the determination of No Carrier Added Specific Activity and the chemical purity of the radiotracer itself. As expected, the real specific activity is lower than the theoretical carrier free one; nevertheless, in most cases, the NCA HSARNs obtained are suitable for purposes envisaged. The use of extra-pure chemicals, targets and equipment allows reaching IDF values in the range from some tens to a few hundreds in some selected cases. Much lower IDF values were obtained with very rare elements.

A method for 3D imaging of absorbed dose in conformal radiotherapy

M. Carrara[1], G. Gambarini [1,2], S. Gay[1,2], L. Pirola[1], and M. Valente[1,2]

1 Dipartimento di Fisica, Università degli Studi di Milano
2 INFN

1. Introduction

In the last decade, technological radiotherapy (RT) improvements have been significant and consequently the use and importance of RT in cancer treatment have greatly increased. A fundamental advance has been the development of external beam techniques aimed at dose deliveries that are highly localised on the tumour volume, sparing at the same time most of the surrounding healthy tissues. These techniques include conformal RT as well as intensity modulated RT (IMRT). However, these methodological improvements require corresponding improvements in the dosimetry methods, in order to ensure that the values calculated with computer treatment planning systems (TPS), adopted in the clinical praxis, agree with the delivered dose distributions. Considering that traditional dosimeters are not well suited to this task, an alternative technique for 3D rendering of in-phantom absorbed dose has been studied and set up.

2. Materials and Methods

In a tissue-equivalent gel matrix, a ferrous sulphate solution and the metal-ion indicator Xylenol Orange (XO) are infused to assess the chemical continuum dosimeter (*gel-dosimeter*). Ionising radiation causes a conversion of ferrous ions Fe^{2+} into ferric ions Fe^{3+}. The complex of XO with Fe^{3+} produces visible light absorption around 585nm, with yield proportional to the absorbed dose. For the analysis, gel dosimeters are placed on a plane light source and transmittance images at 585nm are detected with a CCD camera, before and after their irradiation. Suitable software has been developed, able to carry out all the manipulations necessary to get the interactive rendering of dose profiles, surfaces and volumes, as well as of the isodose curves, starting from a set of acquired transmittance images.

3. Results

After having optimised the protocol for dosimeter preparation and the modality of detecting and manipulating optical images, the method's reliability has been verified. The obtained dose distributions have been compared with those measured by means of a cylindrical ionisation chamber or calculated with Monte Carlo simulations, adopting field geometries in which the last are reliable. After having assured reliability, many experimental configurations in conformal radiotherapy have been verified. As an example, following are reported isodose curves (Fig. 1) and 3D isodose distributions (Fig. 2) obtained in a special configuration of arc therapy. As a qualitative comparison, treatment planning system (TPS) (Prowess 3D) calculations are reported in Fig. 1, as well.

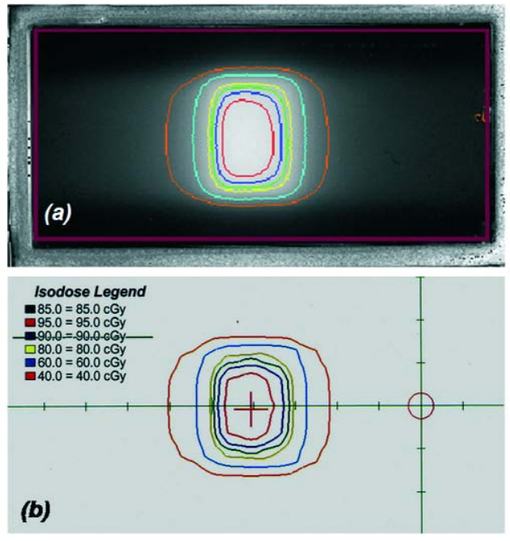

Fig. 1
Relative isodose curves obtained with a single gel-layer (a) and TPS (b) (95% red, 90% blue, 85% green, 80% yellow, 60% light blue, 40% orange)

Fig. 2
3D distribution of relative isodoses
(95% blue, 80% yellow, 40% red)

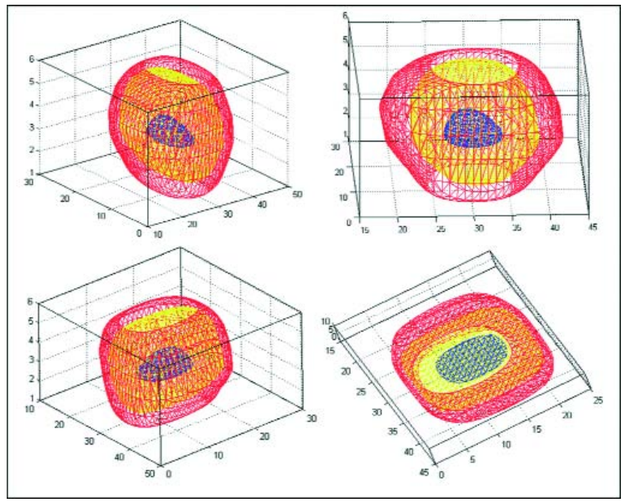

4. Conclusions

The proposed method allows 3D imaging of absorbed dose with high reliability and good spatial resolution.

Development of biokinetic and dosimetric models for incorporation of radionuclides

A. Giussani [1], I. Veronese [1], and M.C. Cantone [1]

1 Dipartimento di Fisica, Università degli Studi di Milano and INFN

The assessment of the internal dose after incorporation of radioactive material requires reliable knowledge of its biokinetics in the human body. The International Commission of Radiological Protection (ICRP) presents, in its Publications, a selection of compartmental models describing absorption into the systemic circulation, transfer between organs and tissues, and excretion for a number of radionuclides and of radioactive compounds. For many substances of radiological relevance, however, lack of sufficiently robust experimental evidence prevents from defining detailed models with specifically determined parameter values. Consequently, the derived dosimetric estimates are of questionable value.

Recent studies with stable tracers conducted by our group have permitted to collect new experimental evidence regarding the biokinetics of elements of radiological relevance. Compartmental analysis approach has been used for interpreting the new pieces of information. In particular, the biokinetic model for radionuclides of molybdenum has been revised on the basis of data collected in a total of more than 50 investigations, and the consequences of this revision on the internal dose estimates have been evaluated [1-5].

Figure 1 shows the structure of the revised model; the new or revised features are indicated in green. Different sets of parameters are recommended in dependence of the chemical form of administration. Non linear kinetics had to be introduced in order to describe the variation of the observed features with mass and modality of administration.

Fig.1
Structure of the revised model for molybdenum

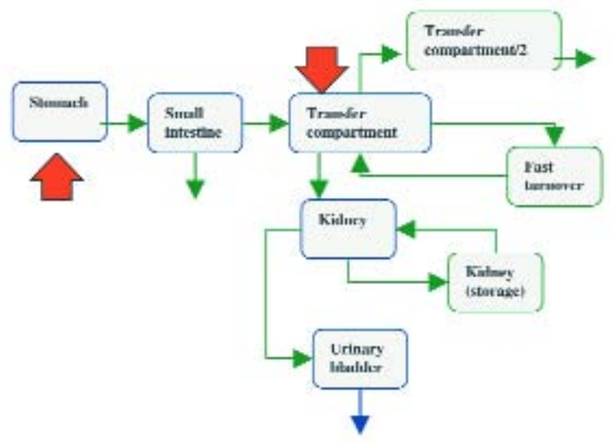

REFERENCES
1. Giussani A. et al.: “A biokinetic model for molybdenum radionuclides: new experimental results” *Radiat. Prot. Dosim.* 79**,** 367-70 (1998).
2. Giussani A. et al.: “A revised model of molybdenum biokinetics in humans for application in radiation protection” *Health Phys.* 75, 479-86 (1998).
3. Giussani A., et al.: “Dosimetry after ingestion of ^{99}Mo radionuclides”. *IV Congreso de Protección Radiológica de Países Europeos del Mediterráneo Occidental*, Barcelona, 27-29 May 1998.
4. Giussani A. et al.: “Internal dose for ingestion of molybdenum radionuclides based on a revised biokinetic model” *Health Phys.*, 78, 46 (2000)
5. Luciani A., et al.: “Sensitivity analysis techniques applied to a revised model of molybdenum biokinetics” *Radiat. Prot. Dosim.* 105, 239 (2003)

Figure 2 shows typical time patterns of the oral tracer, administered in two different forms to the same volunteer and the predictions of the revised model, obtained using specific parameters.

The revised model has also been used for the interpretation of bioassay data from a series of workers who were accidentally exposed to an aerosol containing ^{99}Mo and ^{99m}Tc [6]. Data from experiments with stable tracers have also been used for the validation of the models for radionuclides of ruthenium and zirconium.

Similarly, the compartmental analysis approach was used for the definition of specific pharmacokinetic models for radiopharmaceuticals employed in therapeutic nuclear medicine [7], specifically for ^{131}I as used in the treatment of patients with autonomous functioning thyroid nodule ([8], study conducted in association with Ospedale Maggiore Policlinico, Milano) and for ^{186}Re-HEDP employed for the pain palliation in patients with bone metastases ([9], study conducted in association with Ospedali Riuniti di Bergamo).

Fig. 2
Typical time patterns of the oral tracer and predictions of the revised model.

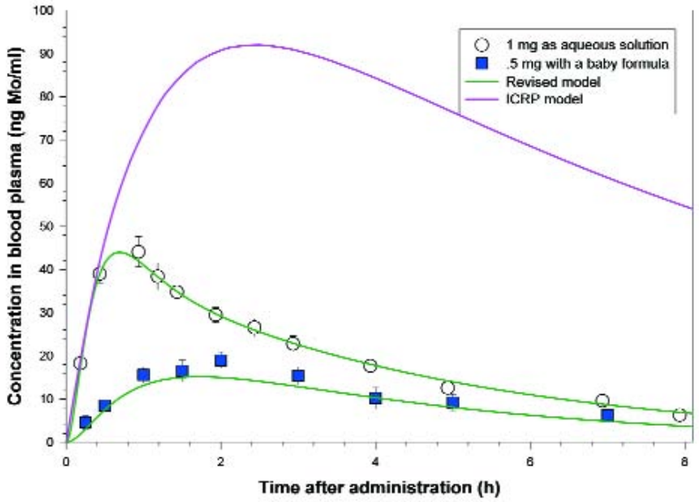

REFERENCES
6. Giussani A. et al.: "Validation of the revised model for the biokinetics of molybdenum with data from a real accidental case" 11th *International Congress of IRPA*, Madrid, 23-28 May 2004.
7. Giussani A. et al.: "Biokinetic assumptions and internal dose estimation in nuclear medicine" 10th *International Congress of the International Radiation Protection Association IRPA-10*, Hiroshima, 14-19 May 2000.
8. Giussani A. et al.: "A compartmental model of the biokinetics of radioiodine in patients suffering from the autonomous thyroid nodule (ATN) syndrome" *European Association of Nuclear Medicine Annual Congress*, Amsterdam, 23-27 August 2003.
9. Giussani A. et al.: "Modelling rhenium distribution and excretion after administration of [^{186}Re]-HEDP for bone pain palliation" *Workshop on Internal Dosimetry of Radionuclides*, Oxford, 9-12 September 2002.

The thermoluminescence peaks of quartz at intermediate temperatures and their use in dating and dose reconstruction

1 Dipartimento di Fisica, Università degli Studi di Milano and INFN

I. Veronese [1], A. Giussani [1], and M.C. Cantone [1]

Introduction

Among the luminescence materials, quartz is one of the most investigated specimens. Generally three main regions can be distinguished in the glow curve: the first consists in only one peak at low temperature, known as "110°C" peak. It was investigated by several authors because of its peculiarity of changing the sensitivity following thermal activation. A second region occurs at temperature higher than 300°C. The glow peaks of this region are known to be thermally stable and are mostly used in TL dating of archaeological manufactures [1]. Between these two regions, quartz exhibits other TL peaks. The sensitivity of these peaks is higher than those occurring at higher temperature, and therefore they are very promising in the assessment of relatively low dose values using samples of recent manufacture. Nevertheless, their employment for dose reconstruction applications requires prior investigations of their luminescent and dosimetric properties, as well as the assessment of the minimum anthropogenic dose detectable using these peaks [2, 3].

The TL peaks of quartz at intermediate temperatures

Figure 1 shows the spectral emission of pure quartz in the temperature range of interest measured using a high sensitive TL spectrometer [4]. Two main peaks (peak I and peak II) occur at temperature of 135°C and 185°C (heating rate 1°C/s) respectively. For both of them the emission band is centred at approximately 380 nm, suggesting the presence of a common recombination centre. The trap parameters of peak I and II were estimated using two different methods of analysis: peak shift (PS) and isothermal decay (ID) [5]. Some results of these analyses are summarised in Table 1.

Fig. 1
Spectral emission of pure quartz (3D vision and contour plot)

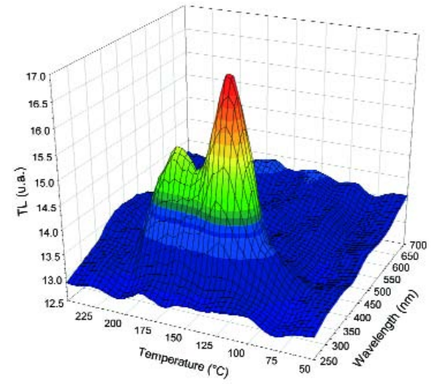

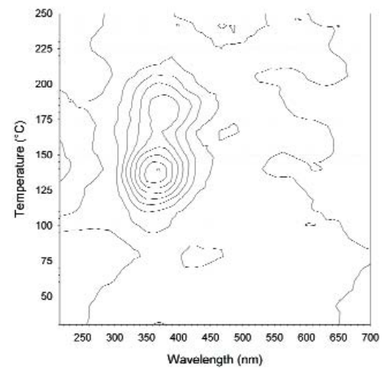

REFERENCES
1. Aitken M.J., *Thermoluminescence dating.* Academic Press, 1985
2. Veronese I., Giussani A., Göksu, H.Y., Martini M., *The trap parameters of electrons in intermediate energy levels in quartz.* Radiat. Meas. 38, 743-6, 2004
3. Veronese I., Giussani A., Göksu, H.Y., Martini M., *Isothermal decay studies of intermediate energy levels in quartz.* Radiat. Environ. Biophys. 43, 51-7, 2004
4. Martini M., Paravisi S. and Liguori C., *A new high sensitivity spectrometer for 3-D thermoluminescence analysis.* Radiat. Prot. Dosim. 66, 447-50, 1996
5. Chen R. and McKeever S.W.S., *Therory of Thermoluminescence and Related Phenomena.* World Scientific, 1997

Limits of thermoluminescence dosimetry

In thermoluminescence dosimetry, the accidental dose Dx can be assessed as the difference between the total accrued dose D_{TL} and the dose due to the natural sources of radiation (alpha, beta, gamma and cosmic rays) absorbed by the sample during its age A:

$$D_x = D_{TL} - A\cdot(N_\alpha + N_\beta + N_\gamma + N_C)$$

Accurate measurements of the terms contributing to Dx and of the uncertainties related to each of them were performed using quartz extracted from one brick and two tiles (50-80 years range) collected from an urban settlement. Independent methods like alpha-counting, beta dosimetry, gamma spectrometry and flame photometry were used for the annual dose assessment. Two approaches were employed for the evaluation of the total accrued dose: regenerative dose and additive dose [1]. The former enables to assess accidental doses as low as approximately 12 mGy by using 10 year old samples, but it can be applied only when sample sensitisation does not occur. The latter can be applied to any sample, however the related uncertainty is higher and minimum detectable anthropogenic dose in young samples amounts to 20 mGy [6].

Table 1
The trap parameters of peak I and II

Peak	Activation energy (eV)	Frequency factor (s^{-1})	Lifetime (at 15°C)	Method of analysis
I	1.13±0.03	$(3.35\pm2.99)\cdot10^{12}$	-	PS
I	1.22±0.02	$(3.39\pm1.46)\cdot10^{13}$	720±70 d	ID
II	1.46±0.06	$(7.79\pm10.91)\cdot10^{14}$	-	PS
II	1.36±0.02	$(2.23\pm0.75)\cdot10^{13}$	580±70 y	ID

REFERENCES
6. Veronese I., Giussani A., Göksu, H.Y., *Limits of thermoluminescence dosimetry using quartz extracted from recent building materials in urban settlements.* J. Env. Rad. 84, 319-39, 2006